9-16-2004

Influence of Equatorial Diatom Processes on Si Deposition and Atmospheric CO(2) Cycles at Glacial/Interglacial Timescales

R. C. Dugdale

M. Lyle

F. P. Wilkerson

Fei Chai
University of Maine - Main, fchai@maine.edu

R. T. Barber

See next page for additional authors

Influence of equatorial diatom processes on Si deposition and atmospheric CO_2 cycles at glacial/interglacial timescales

R. C. Dugdale,[1] M. Lyle,[2] F. P. Wilkerson,[1] F. Chai,[3] R. T. Barber,[4] and T.-H. Peng[5]

Received 19 May 2003; revised 9 June 2004; accepted 2 July 2004; published 16 September 2004

[1] The causes of the glacial cycle remain unknown, although the primary driver is changes in atmospheric CO_2, likely controlled by the biological pump and biogeochemical cycles. The two most important regions of the ocean for exchange of CO_2 with the atmosphere are the equatorial Pacific and the Southern Ocean (SO), the former a net source and the latter a net sink under present conditions. The equatorial Pacific has been shown to be a $Si(OH)_4$-limited ecosystem, a consequence of the low source $Si(OH)_4$ concentrations in upwelled water that has its origin in the SO. This teleconnection for nutrients between the two regions suggests an oscillatory relationship that may influence or control glacial cycles. Opal mass accumulation rate (MAR) data and $\delta^{15}N$ measurements in equatorial cores are interpreted with predictions from a one-dimensional $Si(OH)_4$-limited ecosystem model (CoSINE) for the equatorial Pacific. The results suggest that equatorial Pacific surface CO_2 processes are in opposite phase to that of the global atmosphere, providing a negative feedback to the glacial cycle. This negative feedback is implemented through the effect of the SO on the equatorial $Si(OH)_4$ supply. An alternative hypothesis, that the whole ocean becomes $Si(OH)_4$ poor during cooling periods, is suggested by low opal MAR in cores from both equatorial and Antarctic regions, perhaps as a result of low river input. terminations in this scenario would result from blooms of coccolithophorids triggered by low $Si(OH)_4$ concentrations. *INDEX TERMS:* 1615 Global Change: Biogeochemical processes (4805); 4267 Oceanography: General: Paleoceanography; 3344 Meteorology and Atmospheric Dynamics: Paleoclimatology; 4231 Oceanography: General: Equatorial oceanography; 4805 Oceanography: Biological and Chemical: Biogeochemical cycles (1615); *KEYWORDS:* diatoms, CO_2, silicate

Citation: Dugdale, R. C., M. Lyle, F. P. Wilkerson, F. Chai, R. T. Barber, and T.-H. Peng (2004), Influence of equatorial diatom processes on Si deposition and atmospheric CO_2 cycles at glacial/interglacial timescales, *Paleoceanography*, *19*, PA3011, doi:10.1029/2003PA000929.

1. Introduction

[2] CO_2 increased before the melting of the ice sheets in the last two terminations [*Petit et al.*, 1999] and appears to be a primary driver in glacial cycles [*Shackleton and Pisias*, 1985; *Archer et al.*, 2000]. Interglacial to glacial decreases in atmospheric CO_2 concentration change regularly in step with the Milankovitch solar insolation cycles [*Sigman and Boyle*, 2000]. Although these solar cycles appear to initiate the glacial periods, the decreases in heat input from this source are insufficient to bring about the inferred cooling and glacier formation. Instead they create feedbacks that result in decreased atmospheric CO_2 and increased cooling. *Shackleton* [2000] identified a 100,000 year cycle in ice volume lagging atmospheric temperature, atmospheric CO_2 and deep water temperature, all three found to be in phase with orbital eccentricity, indicating that carbon cycle changes apparently lead the changes in ice volume.

[3] *Broecker* [1982] first proposed that the cause of the CO_2 changes was the oceanic biological pump. His hypothesis would require changes in the nutrient concentrations or supply, since increased nutrients would result in increased new production [*Dugdale and Goering*, 1967] and increased export of carbon to the deep ocean [*Eppley and Peterson*, 1979]) and decreased atmospheric CO_2. In particular increased supply of $Si(OH)_4$ for diatoms, usually considered to be the engines of export production [*Smetacek*, 1998], would be important. Dust deposition, as a source of Si [*Harrison*, 2000], should stimulate diatom productivity. *Archer et al.* [2000] considered that doubling of the $Si(OH)_4$ inventory of the ocean could drive the atmospheric CO_2 changes and glacial cycles, but had difficulty in explaining how the ocean content of $Si(OH)_4$ would have increased by that amount. *Sigman and Boyle* [2000] showed that any credible NO_3 increments would be insufficient to account for the reduction in pCO_2 of 80–100 ppmv that was observed during glacial periods. Also *Loubere* [2000] concluded from carbon isotope data from the foraminiferan *Neogloboquadrina dutertrei* that the Equatorial Undercurrent (EUC) supply of nutrients was lower during the last full glacial (around the Last Glacial Maximum, LGM, 21 kyr) period than at present.

[1] Romberg Tiburon Center, San Francisco State University, Tiburon, California, USA.
[2] Center for Geophysical Investigation of the Shallow Subsurface, Boise State University, Boise, Idaho, USA.
[3] School of Marine Science, University of Maine, Orono, Maine, USA.
[4] NSOE Marine Laboratory, Duke University, Beaufort, North Carolina, USA.
[5] Ocean Chemistry Division, NOAA Atlantic Oceanographic and Meteorological Laboratory, Miami, Florida, USA.

0883-8305/04/2003PA000929

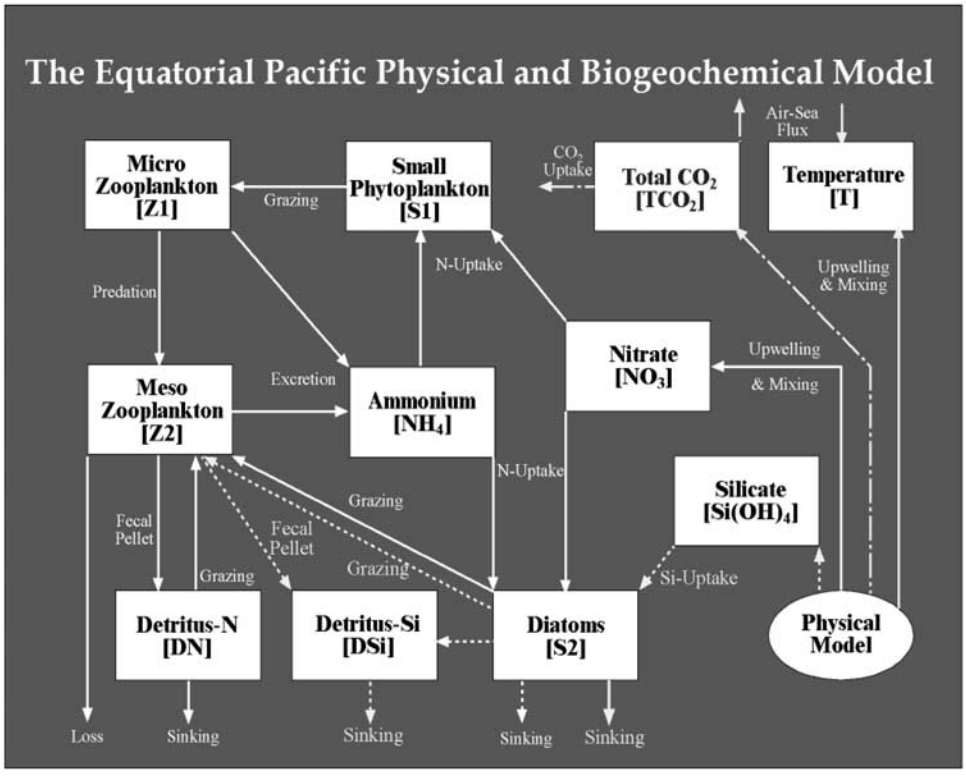

Figure 1. The intercompartmental flow chart of the one-dimensional CoSINE model. The flow of N is indicated by solid line; the flow of Si is indicated by dashed line; and C flow is indicated by line-dashed line.

[4] The two major oceanic regions involved in the glacial to interglacial changes in CO_2 are the equatorial Pacific and Southern Ocean that likely interact to influence the global CO_2 and glacial cycles [e.g., *Brzezinski et al.*, 2002]. The equatorial Pacific is the major ocean region where net CO_2 efflux to the atmosphere occurs [e.g., *Takahashi et al.*, 1986, 1997; *Feely et al.*, 1997] and which has considerable influence on the global carbon budget of the atmosphere. The eastern equatorial Pacific (EEP) upwelling area is considered as a HNLC (high nitrate, low chlorophyll) region due to the presence of considerable NO_3 in the surface waters but low chlorophyll concentration [e.g., *Minas et al.*, 1986; *Dugdale and Wilkerson*, 1998]. The lack of iron (Fe) from atmospheric dust input, was proposed initially as a cause of the incomplete utilization of NO_3 by phytoplankton and hence of surplus CO_2 to be exchanged to the atmosphere from the equatorial Pacific Ocean [e.g., *Chavez et al.*, 1990]. However, *Ku et al.* [1995] using ^{228}Ra showed upwelled $Si(OH)_4$ would be limiting for diatom growth and the equatorial upwelling system has subsequently been designated more accurately as low silicate-HNLC (LSHNLC) [*Dugdale et al.*, 1995]. Confirmation of equatorial $Si(OH)_4$ limitation was obtained from ^{32}Si uptake kinetics [*Leynaert et al.*, 2001]. In this paper we explore the role of equatorial diatoms in Si flux and CO_2 cycles at glacial/interglacial timescales by applying results from an ecosystem model constructed using modern-day data to understand relationships observed in paleoceanographic core data.

[5] Although diatoms in the equatorial upwelling system are low in abundance relative to other non-Si-using phytoplankton [*Bidigare and Ondrusek*, 1996; *Chavez et al.*, 1990]), they may have a dominating effect on other phytoplankton, the nutrient environment and overall productivity. For example, enclosure experiments in a Norwegian fjord showed when $Si(OH)_4$ concentrations were greater than 2 mmol/m^3, diatoms were able to grow faster than the non-Si-users, and inhibited their growth [*Egge and Aksnes*, 1992]. Consideration of interactions between diatoms and other phytoplankton led to the construction of a 1-D biogeochemical model, (CoSINE: carbon, silicate, nitrogen ecosystem model) of the equatorial upwelling system [*Chai et al.*, 2002] (Figure 1). It includes two functional groups of phytoplankton (the numerically dominant small-sized non-Si-using picoplankton, and the Si-requiring diatoms), three nutrients (NO_3, NH_4 and $Si(OH)_4$), two size classes of zooplankton grazers, and detrital N and Si. The influence of Fe is included as a fixed factor reducing photosynthesis below optimal levels. $Si(OH)_4$ and NO_3 are supplied in upwelled water in ratios always less than the 1:1 ratio usually occurring in diatoms [*Brzezinski*, 1985] ensuring that diatom growth will be limited by Si. NO_3, largely unavailable to the picoplankton which primarily use NH_4, will remain in substantial amounts in the surface waters, a well known feature of the eastern equatorial Pacific.

[6] The model can be manipulated to simulate the LSHNLC conditions. One experiment in which the

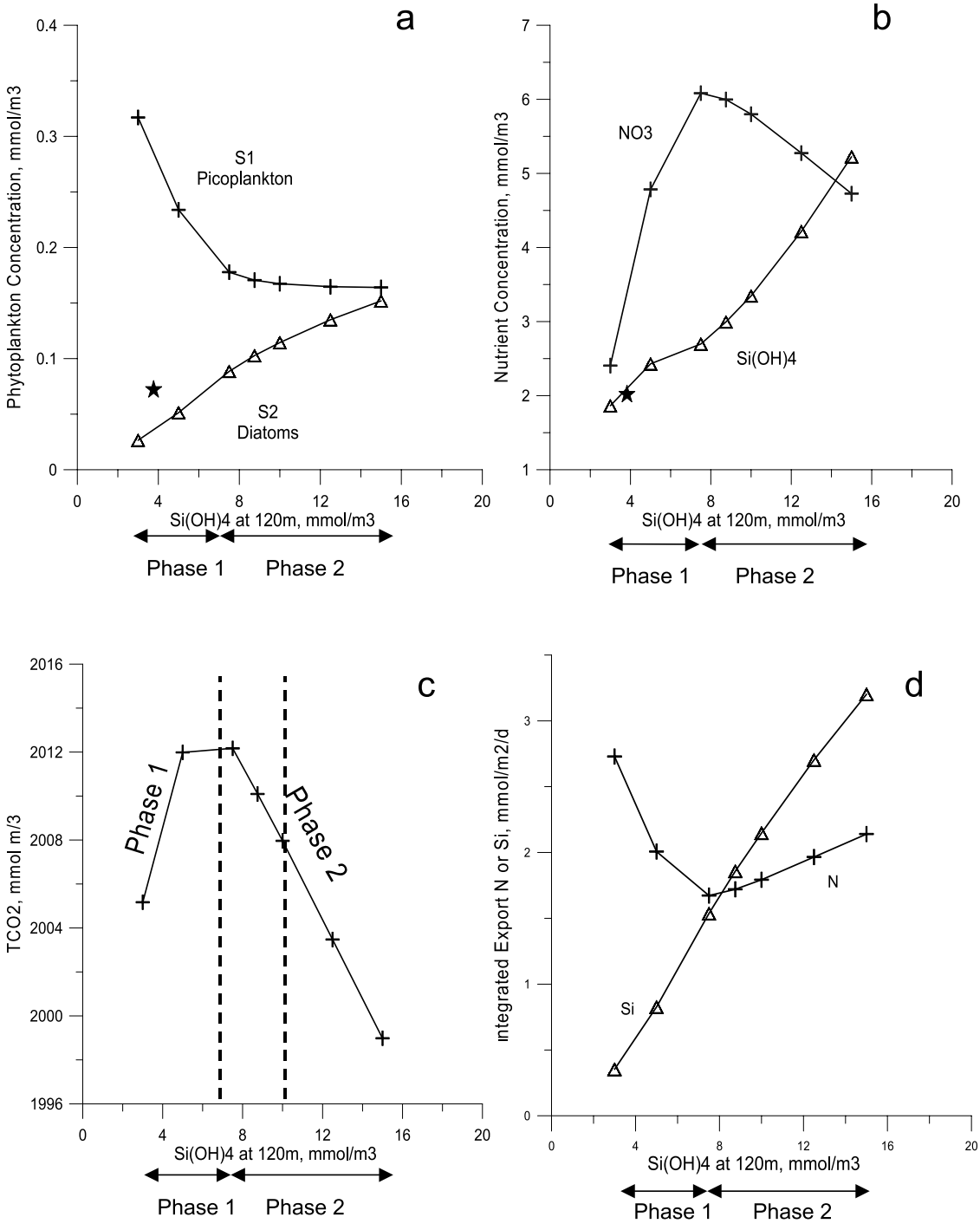

Figure 2. Surface response (phases 1 and 2) of the 1-D CoSINE model to changes in source $Si(OH)_4$ concentration: (a) picoplankton and diatom biomass, mmol/m^3; (b) NO_3 and $Si(OH)_4$ concentrations, mmol/m$^{3;}$, (c) TCO_2, mmol/m^3; (d) integrated export production of N and Si, mmol/m^2/d. Stars are present-day equatorial data from *Leynaert et al.* [2001]. Dotted lines show range of mean $Si(OH)_4$ at 120 m from 140°W, JGOFS.

concentration of $Si(OH)_4$ in the upwelling source waters was increased while holding the NO_3 concentration constant [*Dugdale et al.*, 2002a] showed a two phase response (Figures 2a–2d). The initial response, termed phase 1, is an increase in diatom and decrease in picoplankton biomass (Figure 2a), with accompanying increases in surface nutrient concentrations (Figure 2b), surface TCO_2 (Figure 2c), and Si export (Figure 2d). With a further increase in $Si(OH)_4$ (from 7.5 mmol/m^3 to 15 mmol/m^3), phase 2 then occurs and the biomass of diatoms continues to increase

(Figure 2a), TCO_2 decreases (Figure 2c) and Si export continues to increase linearly with N export increasing slowly relative to Si (Figure 2d). These results represent two extremes: at the lowest $Si(OH)_4$ concentrations the system is fully dominated by picoplankton and at the highest $Si(OH)_4$ concentrations there exists a fully diatom-dominated system. At each extreme, upwelled CO_2 is fully incorporated into the phytoplankton. At intermediate $Si(OH)_4$ concentrations, diatom populations are not sufficiently large to deplete all upwelled CO_2 but are large enough to out-compete picoplankton biomass and their use of CO_2. The existence of a peak in surface TCO_2 (Figure 2c) and NO_3 (Figure 2b) at intermediate $Si(OH)_4$ source concentrations and the linear change of Si export with changes in source $Si(OH)_4$ concentrations (Figure 2d) are the model results to be applied here to explore how diatom driven changes may have resulted in interglacial/glacial changes in atmospheric CO_2. Paleoceanographic and paleoclimate proxy data are re-interpreted in light of these model results to develop a new hypothesis about paleoproductivity and atmospheric CO_2.

2. Differences in Source $Si(OH)_4$ Concentrations to the Equatorial Pacific and the Paleoceanographic Consequences

[7] The primary source for nutrients to the modern Pacific equatorial upwelling ecosystem is the EUC, that is deficient in $Si(OH)_4$ with respect to NO_3 resulting in $Si(OH)_4$ limitation for diatoms [*Ku et al.*, 1995; *Dugdale and Wilkerson*, 1998, 2001; *Leynaert et al.*, 2001; *Jiang et al.*, 2003]. The EUC forms at the western end of the equator where water from the Northern and Southern Hemispheres meet. The contribution of water volume to the EUC is roughly equal between the Northern and Southern Hemispheres. The southern water is low in $Si(OH)_4$ relative to NO_3, while the northern water has about equal concentrations of $Si(OH)_4$ and NO_3 [*Dugdale et al.*, 2002b]. Changes in $Si(OH)_4$ in the Southern Ocean should be reflected in changes in equatorial $Si(OH)_4$ supply and diatom production. In the Southern Ocean, waters strongly deficient in $Si(OH)_4$ compared to NO_3 (i.e. with increased Si trapping) are formed during the austral summer productivity season [*Hiscock et al.*, 2003] and advected northward as Sub-Antarctic Mode Water (SAMW) [*Toggweiler et al.*, 1991; *Dugdale et al.*, 2002b]. Diatomaceous sedimentation rates in the Antarctic, south of the polar front were lower during the last Ice Age [*Sigman and Boyle*, 2000; *Mortlock et al.*, 1991; *Charles et al.*, 1991] suggesting less Si trapping and more $Si(OH)_4$ available for northward transport in the SAMW to the equatorial Pacific: the silicate leakage hypothesis of *Brzezinski et al.* [2002]. If so Southern Ocean productivity can influence equatorial $Si(OH)_4$ concentrations and the Si flux and regulate the resulting CO_2 cycles.

[8] Tropical Pacific cores (central equatorial Pacific, eastern equatorial Pacific, and the Guatemala Basin) [*Lyle et al.*, 1988] exhibit alternating periods of biogenic silica (opal) and carbonate deposition with the major peaks in opal deposition occurring every 100 kyr (the Milankovitch major frequency), suggesting that the supply of $Si(OH)_4$ to the equator has varied in concert with 100 kyr glacial/interglacial cycles. However, high opal burial occurred on the transitions between glacial and interglacial periods, rather than being in phase with either glacial or interglacial periods. To search for a link between glacial equatorial Si burial and changes in atmospheric CO_2, opal deposition from the central equatorial Pacific core W8402-14GC [*Lyle et al.*, 1988] and CO_2 changes from Vostok ice core data [*Petit et al.*, 1999] were compared. We chose to compare W8402-14GC (recovered at 1°N, 139°W) to the ice core record because the largest CO_2 flux from the oceans takes place in the equatorial Pacific between 110° and 160°W [*Takahashi et al.*, 1997]. We assume that $Si(OH)_4$ introduced into surface waters is efficiently incorporated into diatom tests so that the opal rain is a reasonable indicator of $Si(OH)_4$ supply to the surface ocean. We also assume that the majority of opal being deposited in the central equatorial Pacific is of diatom origin. *Murray* [1987] measured the opal flux at a 2-year sediment trap deployment at the location of W8402-14 by partitioning the opal flux into diatom and radiolarian fractions. By using size separations he was able to determine that 75–80% of the total opal flux was of diatom origin. Comparisons of opal flux as determined from the sediment traps with opal sediment deposition [*Dymond and Lyle*, 1985] showed a positive correlation between opal deposition/preservation and opal rain from the surface ocean, perhaps driven, at least in part, by changes in flux of other sedimentary components [*Archer et al.*, 1993]. We also assume that the opal record of W8402-14GC is a reasonable representation of opal deposition in the central equatorial Pacific but recognize that there may be considerable zonal variability, e.g. in the eastern Pacific a 50 kyr opal depositional event is much stronger than to the west [*Lyle et al.*, 1988].

[9] Sediment focusing evaluated by ^{230}Th and ^{3}He may have influenced the apparent burial rates of equatorial sediments [*Marcantonio et al.*, 1996, 2001]. *Marcantonio et al.* [2001] argue that the presence of high concentrations of phytodetritus at the sediment surface from 2°N to 2°S is the result of sediment focusing. However, the latitude band, 2°N to 2°S is the maximum in equatorial upwelling and new production. The simplest explanation is that the phytoplankton blooms resulting from upwelling productivity events are being deposited under the surface where the phytoplankton biomass was produced. The freshness of these deposits argues for a rapid sinking of surface production, a characteristic of diatom blooms in many localities [*Smetacek*, 1985]. In any case W8402-14GC is at a location where *Marcantonio et al.* [1996, 2001] claimed there was no sediment focusing. We are thus inclined to accept the sediment record of biogenic silica (opal) as a record of the overlying productivity, a conclusion based on our understanding of the functioning of the equatorial upwelling system.

[10] The mass accumulation rate of opal (opal MAR) in core W8402-14GC was averaged to 5 kyr intervals (Figure 3). Changes in opal MAR show a strong similarity to changes in atmospheric CO_2, with peak values of both at or near terminations 1 (~12 kyr) and 2 (~130 kyr). These data are combined together in a plot of atmospheric CO_2

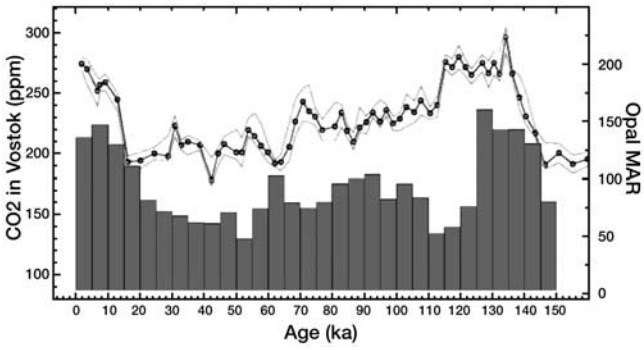

Figure 3. Atmospheric CO_2 (ppmv, single line) from the Vostok core plotted over bar plot of opal mass accumulation rate (mg/cm^2/year) from a central equatorial core (W8402-14GC).

(also averaged to 5 kyr intervals) versus equatorial opal MAR (Figure 4). This plot was made to enable the paleo Si and C trends to be compared with those predicted by the CoSINE model. Opal mass accumulation rate is considered here as a proxy for $Si(OH)_4$ supply or concentration in equatorial source water. If $Si(OH)_4$ source water concentrations varied over glacial cycles in the full range considered in the CoSINE model and the global atmospheric CO_2 concentration varied in phase with the surface TCO_2 at the equator then the CO_2 versus source $Si(OH)_4$ pattern shown in Figure 2c should appear in Figure 4. However, the basic pattern for the core data (Figure 4) is that low opal MAR occurs when Vostok CO_2 is low and high opal MAR occurs when CO_2 is high; i.e. the relationship between opal MAR and global atmospheric CO_2 is almost always positive. There is no evidence from the relationship of global atmospheric CO_2 and opal MAR of a phase 2 limb that would appear to the right in Figure 4 at the high opal MAR values and with negative slope. While it is tempting to interpret the data in Figure 4 as indicating a model phase 1 at the equator, the conclusion would only be valid if the changes in TCO_2 at the equator were in phase with the global atmosphere changes and we have no evidence for such an in-phase condition. Consequently Figure 4 can only be used to indicate that equatorial opal MAR appears to have a positive relationship with the global atmosphere CO_2 changes.

3. Paleoceanographic Nutrient Conditions Resolved by Natural Isotope Abundances

[11] Variations in the natural abundance of N, C and Si isotopes in core material provide another tool for understanding paleoceanographic nutrient conditions, [*Farrell et al.*, 1995; *Altabet and Francois*, 1994]. The basis for the method is the fractionation of isotope pairs, e.g. $^{15}N/^{14}N$, $^{13}C/^{12}C$, $^{30}Si/^{28}Si$ during phytoplankton uptake and assimilation. Although various outcomes are possible depending on the particular environmental conditions, the change in isotope composition depends on the degree of utilization of the element [*Altabet and Francois*, 1994] such that as available nutrient is reduced to near source levels, the isotope composition of the phytoplankton becomes heavier by Rayleigh fractionation. In the case of nitrogen this is expressed as an increase in $\delta^{15}N$ and occurs with decreased NO_3 concentration.

[12] Our analysis suggests the equatorial upwelling system experienced decreased source $Si(OH)_4$ supply (i.e. low opal MAR) over most of the last cooling cycle,125–25 kyr (Figure 4) i.e. model phase 1. The CoSINE model output can also be used to predict changes in utilization of NO_3 and $Si(OH)_4$ and changes in $\delta^{15}N$ as a function of source $Si(OH)_4$ (Figures 5a and 5b). $\delta^{15}N$ natural abundance variations were obtained from CoSINE model predicted values of surface NO_3 by calculating the relative NO_3 utilization (Figure 5a), as the difference between the 120 m source NO_3 (12 mmol/m^3, held constant in the model) and the surface NO_3 concentration divided by the source NO_3 concentration as the 120 m source $Si(OH)_4$ was varied (Figure 2b) and inserting that value into *Altabet* [2001, equation (4)] for first order Rayleigh fractionation. The model predicts a U-shaped curve (Figure 5b) with a minimum in $\delta^{15}N$ at the transition between phase 1 and 2. *Farrell et al.* [1995] measured nitrogen isotope ratios in bulk nitrogen in three cores from the eastern equatorial Pacific. Their $\delta^{15}N$ measurements cover the periods, 24–12 kyr including the LGM, termination 1 (12 kyr), and 12–0 kyr warming (Holocene). Minimum values occurred at the LGM and increased toward the Holocene. *Farrell et al.* [1995] attributed low $\delta^{15}N$ values at the LGM to an elevated NO_3 supply to the euphotic zone due to increased upwelling apparently without a compensating increase in NO_3 uptake (new production). However, the CoSINE model results suggest that the low $\delta^{15}N$ at the LGM was due to low

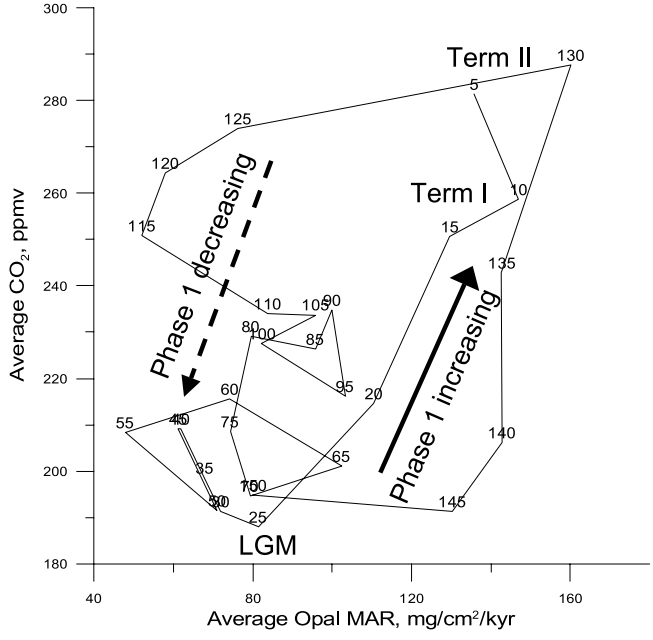

Figure 4. Average atmospheric CO_2 (ppmv) from the Vostok core plotted against average opal MAR (mg/cm^2/year) from the equatorial core labeled with numbers indicating age in kiloyears.

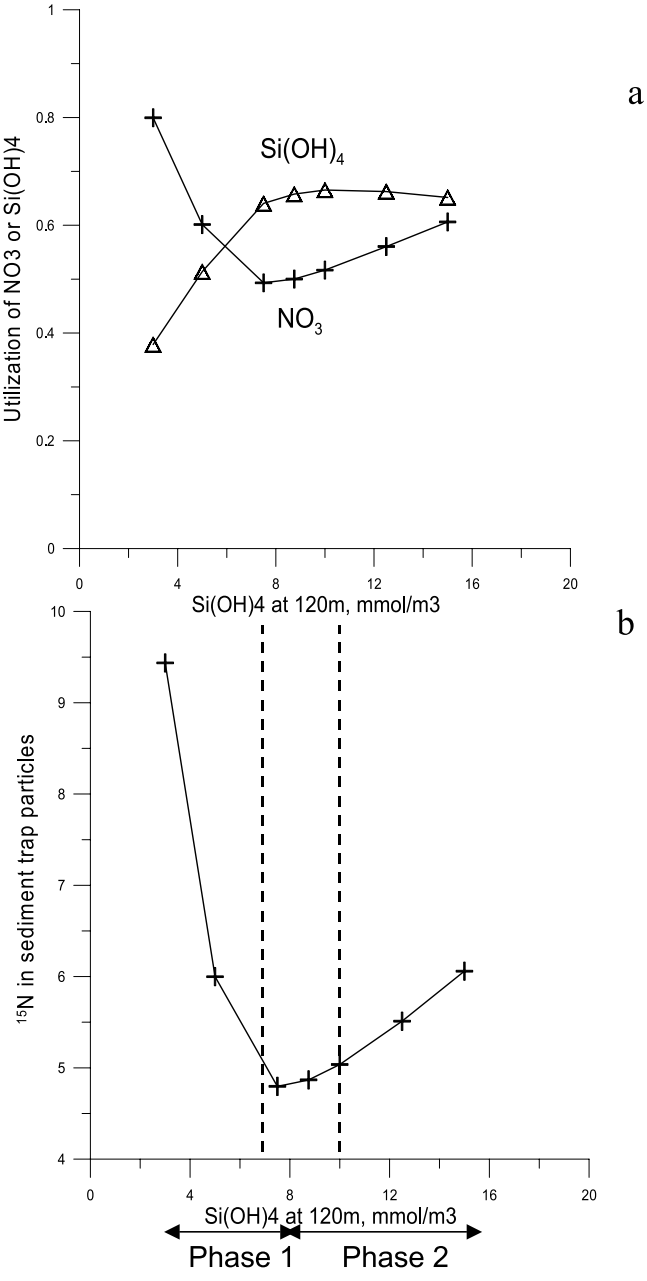

Figure 5. (a) Modeled utilization of NO_3 or $Si(OH)_4$ and (b) modeled $\delta^{15}N$ in trap particles versus source $Si(OH)_4$ concentration computed with CoSINE model and *Altabet* [2001, equation (4)]. Dotted lines show range of mean $Si(OH)_4$ at 120 m from 140°W, U.S. JGOFS.

$Si(OH)_4$ supply to the equator resulting in high unused NO_3 (Figure 2b), rather than to an increase in NO_3 supply. The subsequent increase in $\delta^{15}N$ was due to an improved $Si(OH)_4$ supply. The minimum in $\delta^{15}N$ during the LGM may represent the transition point in Figure 5b, between model phases, which is also the point of maximum surface TCO_2 (Figure 2c). The range of mean $Si(OH)_4$ concentrations at 120 m measured on U.S. JGOFS cruises to 140°W [*Dugdale et al.*, 2002a, Table 2] are shown as vertical lines in Figures 2 and 5. This range of contemporary source $Si(OH)_4$ concentrations along with indications of increasing export of Si at the equator (Figure 3) from the LGM to the Holocene are consistent with the CoSINE results suggesting a transition from phase 1 to phase 2. The evidence from $\delta^{15}N$ analyses of equatorial cores interpreted with the CoSINE model suggests the LGM was at the transition point between phase 1 and phase 2. Increased $Si(OH)_4$ flux to the sediments from the glacial minima to the transitions combined with CoSINE results also point to phase 2 changes as suggested by the vertical lines in Figures 2 and 5. The CoSINE model and $\delta^{15}N$ results indicate a maximum in TCO_2 at the equator at the glacial maximum, specifically the LGM, and at that time the equator would have been a maximum source to the atmosphere. However, low equatorial opal MAR correlates with low global atmospheric CO_2 and high equatorial MAR opal with high atmospheric CO_2 suggesting that the equator is out of phase with some other process influencing atmospheric CO_2 in an opposite way. The suggestion of maximum CO_2 flux to the atmosphere at the equator during glacial periods is consistent with the analysis of *Pedersen et al.* [1991] who suggest cooler temperatures and higher CO_2 flux to the atmosphere for the eastern equatorial Pacific over the last 30 kyr.

[13] *Altabet* [2001] obtained $\delta^{15}N$ values from a JGOFS core at 0°, 140°W, within a degree of where W8402-14GC was collected. The $\delta^{15}N$ values have cyclic saw-tooth like changes over the last 600 kyr with a periodicity of ~100 kyr [*Altabet*, 2001] (Figure 6). The period recorded by this core includes both termination 2 and termination 1. Both terminations are periods of increasing opal MAR (Figures 3 and 4a). The rapid rise in $\delta^{15}N$ from 150–125 kyr, which includes termination 2 (128 kyr) is correlated with an increase in opal MAR. The rapid decrease from 125–110 kyr coincides with a decrease in opal MAR. The period from 25–0 kyr which includes the LGM (21 kyr) and termination 1 (12 kyr) is also a period of rapid increase in opal MAR (Figure 3) and increasing $\delta^{15}N$. In both terminations, the positive relationship between opal MAR and $\delta^{15}N$ suggests model phase 2 conditions, in agreement with the termination 1 data from *Farrell et al.* [1995]. *Altabet* [2001] interpreted increases in $\delta^{15}N$; i.e. increased NO_3

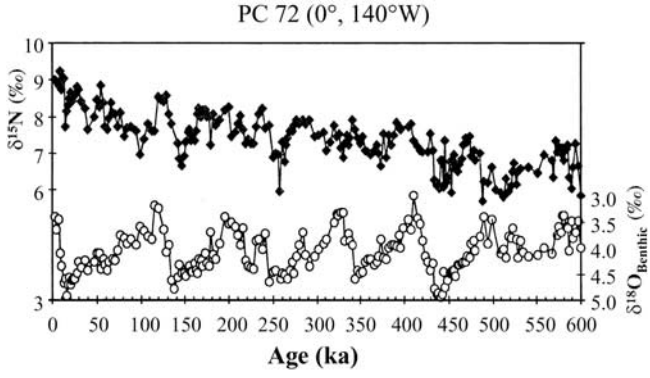

Figure 6. Bulk sediment $\delta^{15}N$ at the equator for the last 600 kyr from Piston core PC 72 collected during U.S. JGOFS EqPac Program [from *Altabet*, 2001, Figure 11].

utilization as a consequence of increased Fe availability and higher new production. However, the changes predicted by the CoSINE model are consistent with the *Altabet* [2001] N isotope measurements and provide an alternate explanation, i.e., increased $\delta^{15}N$ is due to increased $Si(OH)_4$ supply resulting in increased NO_3 utilization.

4. Hypothetical Si-Driven Glacial Cycle

[14] The equatorial Pacific is a chronically $Si(OH)_4$-limited ecosystem receiving $Si(OH)_4$ from the Southern Ocean through SAMW that is rich in NO_3 and low in $Si(OH)_4$. Our modeling shows $Si(OH)_4$-limited diatoms to control the success of other non-Si-using phytoplankton in the equatorial ecosystem in such a way that a bell shaped curve emerges of surface TCO_2 as a function of $Si(OH)_4$ source concentration (Figure 2c). For the cores considered here, the relationship between Si deposition and Vostok atmospheric CO_2 appears to be always positive. Interpretation of this pattern requires recognition that although the opal MAR represents local equatorial processes, the atmospheric CO_2 values are global, the result of both local and remote processes. If we take the $\delta^{15}N$ isotope data to indicate the equator is in model phase 2 (increasing and decreasing source $Si(OH)_4$ over glacial cycles) then when source $Si(OH)_4$ is low, $\delta^{15}N$ is low and equatorial TCO_2 is highest (Figure 2). However, at low source $Si(OH)_4$ concentrations, global atmospheric CO_2 is at a minimum (Figure 4), indicating the equatorial CO_2 cycle is in opposite phase to global atmospheric CO_2. The link between Southern Ocean and equatorial $Si(OH)_4$ biogeochemical processes provides a negative feedback in the warming and cooling cycle. In a cooling period the Southern Ocean exhibits high diatom productivity, high CO_2 influx from the atmosphere; $Si(OH)_4$ export to the equator is reduced. As equatorial diatom productivity declines due to reduced source $Si(OH)_4$, equatorial CO_2 flux to the atmosphere increases. At some point equatorial CO_2 flux becomes dominant over Southern Ocean CO_2 absorption and warming begins. In an alternative scenario, as equatorial $Si(OH)_4$ continues to decline, the equatorial system enters model phase 1 and CO_2 changes in the surface waters are in synchrony with the Southern Ocean resulting in a rapid decline in atmospheric CO_2 leading to full glacial conditions. When a critical low source $Si(OH)_4$ concentration is reached, blooms of coccolithophorids are triggered [*Aksnes et al.*, 1994], releasing CO_2 to the surface waters and to the atmosphere. The equator has been converted from a sink to a source of atmospheric CO_2. Warming begins rapidly with increased $Si(OH)_4$ supply to the ocean, e.g. from river input and glacial melting and the cycle begins again. In this scenario, the equator is initially a brake on decreasing atmospheric CO_2, later falls into synchrony with the Southern Ocean and finally triggers rapid CO_2 release and warming.

5. Causes of the Changes in Source $Si(OH)_4$

[15] This hypothetical cycle based upon the CoSINE model simulations, is driven by changes in $Si(OH)_4$ supply to the equatorial Pacific. The causes of the changes in $Si(OH)_4$ supply, besides the reduced supply from the Southern Ocean to the EUC, include weathering, glacial melting, drying of the climate, river inputs and dust. Rapid increases in opal MAR and CO_2 occurred from 150–135 kyr, just prior to termination 2 (128 kyr), and 35–5 kyr including the LGM and termination 1. CO_2 and air temperature are in phase with the 100,000 year ice age cycle, but changes in ice volume lags both [*Shackleton*, 2000]. Since opal MAR changes in the central equatorial core are in phase with CO_2, ice volume also lags opal MAR in this case. The lag in ice volume change, i.e. melting, eliminates increased weathering and also glacial melting with inputs of glacial flour [*Pollock*, 1997] as the sources of increased $Si(OH)_4$ at the terminations. Re-dissolution from the continental shelf sediments does not appear to be a viable source of $Si(OH)_4$ since CO_2 rose before sea level increased at terminations [*Broecker and Henderson*, 1998]. The dust pulses shown in the work of *Petit et al.* [1999, Figure 2], occurred also with a 100 kyr frequency but declined to low levels just before the rise in air temperature and CO_2 at termination 2, the "demise of the dust" [*Broecker and Henderson*, 1998]. The low dust period lasted until about 60 kyr. Although aeolian inputs of Si are only about 10% of river inputs [*Tréguer et al.*, 1995], the dust falls on the surface and can have an immediate effect on the euphotic zone. However, the high dust period precedes the increase in Si deposition at termination 2 and so is unlikely to be the source of increased Si at terminations.

[16] Another possible explanation for decreasing input of $Si(OH)_4$ to the ocean is a progressive drying of the climate which would affect both the inputs of $Si(OH)_4$ from both local, western Pacific rivers, and to the EUC from both the Northern and Southern Hemispheres. River inputs are the primary source of $Si(OH)_4$ ($\sim$90%) to the modern ocean, with hydrothermal vents and basalt dissolution making up the remaining 10% [*Tréguer et al.*, 1995]. Input from the North Pacific would be affected both directly through lower river $Si(OH)_4$ supply to the ocean and perhaps by a decrease in the estuarine effect with deepening of the nutricline. $Si(OH)_4$ input from the rivers of the western tropical Pacific [*Dugdale et al.*, 2002b] would decrease with the drying of the climate. The southern source of $Si(OH)_4$ to the EUC would also be reduced by reduced river input to the Atlantic and Indian Oceans. A shutdown or decrease in the conveyer belt transporting nutrients in deep water from the Atlantic toward the south would also starve the Southern Ocean of $Si(OH)_4$. The timescales for precipitation induced changes to the Si budget of the world oceans would be somewhere close to the turnover time for $Si(OH)_4$ as a function of river input, about 15,000 years [*Tréguer et al.*, 1995] and so match the timescale of the slow equatorial opal decline. During the long cooling phase (107–23 kyr), Southern Ocean productivity south of the polar front declined; a fourfold decrease according to *Mortlock et al.* [1991] and *Charles et al.* [1991], but this reduction in southern Si demand did not result in increased export to the equator. On balance, at least the regions south of the polar front in the Southern Ocean were starved of $Si(OH)_4$ along with the equatorial system.

[17] Decreased $Si(OH)_4$ and opal accumulation during interglacial cooling, might also occur if the global supply of $Si(OH)_4$ became progressively sequestered in the coastal margins [*Berger et al.*, 1994]. *Berger et al.* [1994] observed that the global ocean must have had a very different chemistry during periods of glacial accumulation. However, the diatom record from cores taken from three Atlantic coastal upwelling sites [*Abrantes*, 2000] shows the same pattern as the equatorial Pacific and the Southern Ocean, i.e. very low opal accumulation during the post termination 2 interglacial period with large accumulations beginning in isotope stage 2 and reaching peak values in termination 1. The apparent global decline of $Si(OH)_4$ as indicated by core opal in upwelling areas during cooling periods may be a result of the silicate pump [*Dugdale and Wilkerson*, 1998; *Ragueneau et al.*, 2002]. $Si(OH)_4$ is efficiently exported from the euphotic zone through its low regeneration rate compared to N or P [*Dugdale et al.*, 1995]. The relatively low dissolution rate of diatom frustules compared to water column regeneration of N and P drives upwelling systems with diatom populations into $Si(OH)_4$ limitation, leaving behind relatively high levels of N and P. The consequence of silicate pumping is that the marine Si cycle is more reactive to changes in inputs than N, which is recycled biologically at a rapid rate and which has a new source in biological nitrogen fixation. Global marine nitrogen fixation is now recognized to be a significant part of the oceanic N budget [*Karl et al.*, 2002]. As a consequence, a certain level of uncoupling between Si and N on the glacial timescale is likely to occur. The Si cycle should be strongly dependent on climate related changes in weathering and runoff but the highly biological nitrogen cycle is less affected.

6. Discussion

[18] We have shown that equatorial Pacific cores show low opal deposition in interglacial periods when CO_2 is low, increasing opal MAR at glacial maxima and high opal deposition at terminations when atmospheric CO_2 is high. Cores north of the polar front in the Southern Ocean and Atlantic coastal upwelling areas [*Abrantes*, 2000] also show the same pattern, as do cores from the California margin [*Kienast et al.*, 2002; *Lyle et al.*, 1992; *Gardner et al.*, 1997], consistent with the pattern predicted and recreated by the 1-D CoSINE model for low source $Si(OH)_4$ concentrations, i.e., phase 1 [*Dugdale et al.*, 2002a]. In the model this direct relationship between source $Si(OH)_4$ and surface TCO_2 is the result of diatom suppression of non-Si-requiring phytoplankton.

[19] The Southern Ocean has been suggested as a source of the varying Si deposition in the equatorial region, through decreased Si trapping during glacial periods communicated as increased $Si(OH)_4$ to the equator through advection of SAMW to the EUC [*Dugdale et al.*, 2002a], and the silicate leakage hypothesis [*Brzezinzki et al.*, 2002]. The present study however, suggests that Antarctic and equatorial changes in opal MAR vary together. Alternatively, the supply of $Si(OH)_4$ remains constant during glacial cycles, but is re-distributed between different parts of the Southern Ocean and equatorial systems. However, it may emerge that different regions of the equatorial/southern ocean system are in different, opposite deposition phases, e.g. the more direct effect of the SAMW water may be to the eastern equatorial Pacific, through the lower EUC which transits under the equatorial upwelling system, upwells along the Peru coast and turns north to supply some of the water to the EEP upwelling system [*Toggweiler and Carson*, 1995; *Dugdale et al.*, 2002b]. The upper part of the EUC is supplied from shallower waters to the south and north and so is less influenced by SAMW water. In this case, the pattern of Si deposition in the central and eastern equatorial Pacific could be either in or out of phase with each other. Enhanced export production north of the polar front during glacial periods would send water with decreased Si concentration northward. Additional studies of opal deposition in both equatorial and Antarctic cores will be useful in corroborating or refuting the silicate leakage hypothesis, the general conclusion of *Berger et al.* [1994] and our results suggesting that opal deposition tends to be low in glacial periods.

[20] We have interpreted variations in natural abundance of N, Si and C isotopes from the equatorial Pacific and our model results to indicate that the equatorial Pacific provides a negative feedback on CO_2 processes in the Southern Ocean. Additional measurements of stable isotope natural abundances in cores from the two regions would allow further tests of the hypothesis that variations in Si and N isotopes are the result of changes in $Si(OH)_4$ supply rather than changes in Fe or other drivers of enhanced production. The possibility that low $Si(OH)_4$ conditions are necessary for the blooming of coccolithophorids, adds another dimension to the hypothesis that variations in $Si(OH)_4$ supply during glacial/interglacial cycles affect the emission of CO_2 through diatom control of upwelling ecosystem functioning. *Dymond and Lyle* [1985] suggested that a reduction in the proportion of diatoms to coccolithophorids would lead to more calcite export from the equatorial surface waters and an increase in CO_2. An attractive element of this hypothesis is that it predicts the alternating opal-rich and carbonate-rich deposits under the equatorial Pacific.

[21] The purpose of this study was to add a new biological dimension and new theory to the quest for understanding glacial CO_2 cycles. Our major conclusion from data and modeling is that the role of diatoms in carbon export needs to be considered in a more complex way than the commonly accepted mode where increased diatom production equals increased carbon export. At low $Si(OH)_4$ source levels, diatom interaction with other non-Si-requiring phytoplankton may have the counter-intuitive result that increased $Si(OH)_4$ source concentration and increased diatom populations result in greater surface TCO_2 concentrations and increased evasion of CO_2 to the atmosphere. At even higher $Si(OH)_4$ source concentrations, increased diatom populations result in lower TCO_2 and decreased CO_2 flux to the atmosphere. Although the changes in TCO_2 in equatorial surface waters predicted by the CoSINE model are relatively small, they are enough to change the equator from a net source to a net sink and so lead to a new equilibrium value for the atmosphere. The possibility that the equatorial Pacific may provide either negative or positive feedback

to Southern Ocean processes is intriguing. The observed relationship between $Si(OH)_4$ deposition and glacial/interglacial CO_2 may be causal or artifact, but in any case should be considered in the context of climate changes on short or long timescales. Of particular interest is the question of the source of increased $Si(OH)_4$ just prior to or at terminations. Field studies to test these model driven hypotheses need to be made in the equatorial Pacific. We hope some contribution will be made by these efforts to the puzzle of glacial/interglacial feedback systems in Earth's biogeochemical system.

[22] **Acknowledgments.** We wish to thank the National Science Foundation for financial support to R. Dugdale and F. Wilkerson (JGOFS-Synthesis and Modeling Program (SMP) grant OCE-01354430), F. Chai (SMP OCE-137272), and M. Lyle (OCE-9811272 and EPS 0132626). We would like to dedicate this paper to Jack Dymond, a close friend and colleague. His insights into biogeochemical cycling will be missed by us all. This is US JGOFS contribution 1048.

References

Abrantes, F. (2000), 200,000 yr diatom records from Atlantic upwelling sites reveal maximum productivity during LGM and a shift in phytoplankton community structure at 185,000 yr, *Earth Planet. Sci. Lett.*, *176*, 7–16.

Aksnes, D. L., J. K. Egge, R. Rosland, and B. R. Heimdal (1994), Representation of *Emiliania huxleyi* in phytoplankton simulation models: A first approach, *Sarsia*, *79*, 291–300.

Altabet, M. (2001), Nitrogen isotopic evidence for micronutrient control of fractionated NO_3 utilization in the equatorial Pacific, *Limnol. Oceanogr.*, *46*, 368–380.

Altabet, M., and R. Francois (1994), The use of nitrogen isotopic ratio for reconstruction of past changes in surface ocean nutrient utilization, *NATO ASI Ser.*, *17*, 281–305.

Archer, D. E., M. Lyle, K. Rodgers, and P. Froelich (1993), What controls opal preservation in tropical deep-sea sediments, *Paleoceanography*, *8*(1), 7–21.

Archer, D. E., A. Wingruth, D. Lea, and N. Mahowald (2000), What caused the glacial/interglacial atmospheric pCO_2 cycles, *Rev. Geophys.*, *38*, 159–190.

Berger, W. H., J. C. Herguera, C. B. Lange, and R. Schneider (1994), Paleoproductivity: Flux proxies versus nutrient proxies and other problems concerning the quaternary productivity record, *NATO ASI Ser.*, *17*, 385–412.

Bidigare, R. R., and M. E. Ondrusek (1996), Spatial and temporal variability of phytoplankton pigment distributions in the central equatorial Pacific Ocean, *Deep Sea Res. Part II*, *43*, 809–833.

Broecker, W. S. (1982), Ocean chemistry during glacial time, *Geochim. Cosmochim. Acta*, *46*, 1689–1706.

Broecker, W. S., and G. M. Henderson (1998), The sequence of events surrounding termination II and their implications for the cause of glacial-interglacial CO_2 changes, *Paleoceanography*, *13*(4), 352–364.

Brzezinski, M. A. (1985), The Si:C:N ratio of marine diatoms: Interspecific variability and the effect of some environmental variables, *J. Phycol.*, *21*, 347–357.

Brzezinski, M. A., C. J. Pride, V. M. Franck, D. M. Sigman, J. L. Sarmiento, K. Matsumoto, N. Gruber, G. H. Rau, and K. H. Coale (2002), A switch from $Si(OH)_4$ to NO_3 depletion in the glacial Southern Ocean, *Geophys. Res. Lett.*, *29*(12), 1564, doi:10.1029/2001GL014349.

Chai, F., R. C. Dugdale, T.-H. Peng, F. P. Wilkerson, and R. T. Barber (2002), One-dimensional ecosystem model of the equatorial Pacific upwelling system, part I: Model development and silicon and nitrogen cycle, *Deep Sea Res. Part II*, *49*, 2713–2745.

Charles, C. D., P. N. Froelich, M. A. Zibello, R. A. Mortlock, and J. J. Morley (1991), Biogenic opal in southern ocean sediments over the last 450,000 years: Implications for surface water chemistry and circulation, *Paleoceanography*, *6*, 697–728.

Chavez, F. P., K. R. Buck, and R. T. Barber (1990), Phytoplankton taxa in relation to primary production in the equatorial Pacific, *Deep Sea Res.*, *37*, 1733–1752.

Dugdale, R. C., and J. J. Goering (1967), Uptake of new and regenerated forms of nitrogen in primary productivity, *Limnol. Oceanogr.*, *12*, 196–206.

Dugdale, R. C., and F. P. Wilkerson (1998), Silicate regulation of new production in the equatorial Pacific upwelling, *Nature*, *391*, 270–273.

Dugdale, R. C., and F. P. Wilkerson (2001), Sources and fates of silicon in the ocean: the role of diatoms in climate and glacial cycles, *Sci. Mar.*, *65*(suppl. 2), 141–152.

Dugdale, R. C., F. P. Wilkerson, and H. J. Minas (1995), The role of a silicate pump in driving new production, *Deep Sea Res. Part I*, *42*, 697–719.

Dugdale, R. C., R. T. Barber, F. Chai, T.-H. Peng, and F. P. Wilkerson (2002a), One-dimensional ecosystem model of the equatorial pacific upwelling system, part II: Sensitivity analysis and comparison with JGOFS EqPac data, *Deep Sea Res. Part II*, *49*, 2747–2768.

Dugdale, R. C., A. G. Wischmeyer, F. P. Wilkerson, R. T. Barber, F. Chai, M. Jiang, and T.-H. Peng (2002b), Meridional asymmetry of source nutrients to the equatorial Pacific upwelling ecosystem and its potential impact on ocean-atmosphere CO_2 flux: A data and modeling approach, *Deep Sea Res. Part II*, *49*, 2513–2531.

Dymond, J., and M. Lyle (1985), Flux comparisons between sediments and sediment traps in the eastern tropical Pacific: Implications for atmospheric CO_2 variations during the Pleistocene, *Limnol. Oceanogr.*, *30*, 699–712.

Egge, J. K., and D. L. Aksnes (1992), Silicate as a regulating nutrient in phytoplankton competition, *Mar. Ecol. Progr. Ser.*, *83*, 281–289.

Eppley, R. W., and B. J. Peterson (1979), Particulate organic matter flux and planktonic new production in the deep ocean, *Nature*, *282*, 677–680.

Farrell, J. W., T. F. Pedersen, S. E. Calvert, and B. Nielsen (1995), Glacial-interglacial changes in nutrient utilization in the equatorial Pacific Ocean, *Nature*, *377*, 514–517.

Feely, R. A., R. Wanninkhof, C. Goyet, D. E. Archer, and T. Takahashi (1997), Variability of CO_2 distributions and sea-air fluxes in the central and eastern equatorial Pacific during the 1991–1994 El Niño, *Deep Sea Res. Part II*, *44*, 1851–1867.

Gardner, J. V., W. E. Dean, and P. Dartnell (1997), Biogenic sedimentation beneath the California Current system for the past 30 kyr and its paleoceanographic significance, *Paleoceanography*, *12*, 207–227.

Harrison, K. G. (2000), Role of increased marine silica input on paleo-pCO_2 levels, *Paleoceanography*, *15*, 292–298.

Hiscock, M. R., J. Marra, W. O. Smith Jr., R. Goericke, C. Measures, S. Vink, R. J. Olson, H. M. Sosik, and R. T. Barber (2003), Primary productivity and its regulation in the Pacific Sector of the Antarctic Circumpolar Current, *Deep Sea Res. Part II*, *50*, 533–559.

Jiang, M., F. Chai, R. T. Barber, R. C. Dugdale, F. P. Wilkerson, and T.-H. Peng (2003), A nitrate and silicate budget in the equatorial Pacific Ocean: A coupled biological-physical model study, *Deep Sea Res. Part II*, *50*, 2971–2996.

Karl, D., A. Michaels, B. Bergman, D. Capone, E. J. Carpenter, R. Letelier, F. Lipschultz, H. Paerl, D. Sigmon, and L. Stal (2002), Dinitrogen fixation in the world's oceans, *Biogeochemistry*, *57–58*, 47–98.

Kienast, S. S., S. E. Calvert, and T. F. Pedersen (2002), Nitrogen isotope and productivity variations along the northeast Pacific margin over the last 120 kyr: Surface and subsurface paleoceanography, *Paleoceanography*, *17*(4), 1055, doi:10.1029/2001PA000650.

Ku, T. L., S. Luo, M. Kusakabe, and J. K. B. Bishop (1995), ^{228}Ra-derived nutrient budgets in the upper equatorial Pacific and the role of "new" silicate in limiting productivity, *Deep Sea Res. Part II*, *42*, 479–497.

Leynaert, A., P. Tréguer, C. Lancelot, and M. Rodier (2001), Silicon limitation of biogenic silica production in the equatorial Pacific, *Deep Sea Res.*, *48*, 639–660.

Loubere, P. (2000), Nutrient and oceanographic changes in the eastern equatorial Pacific from the last full glacial to the present, *Global Planet. Change*, *29*, 77–98.

Lyle, M., D. W. Murray, B. P. Finney, J. Dymond, J. M. Robbins, and K. Brooksforce (1988), The record of Late Pleistocene biogenic sedimentation in the eastern tropical Pacific Ocean, *Paleoceanography*, *3*, 39–59.

Lyle, M., R. Zahn, F. Prahl, J. Dymond, R. Collier, N. Pisias, and E. Suess (1992), Paleoproductivity and carbon burial across the California Current: The MULTITRACERS transect, 42°N, *Paleoceanography*, *7*, 251–272.

Marcantonio, F., R. F. Anderson, M. Stute, N. Kumas, P. Schlosser, and A. Mix (1996), Extraterrestrial ^{3}He as a tracer of marine sediment transport and accumulation, *Nature*, *383*, 705–707.

Marcantonio, F., R. F. Anderson, S. Higgins, M. Stute, P. Schlosser, and P. Kubik (2001),

Sediment focusing in the central equatorial Pacific Ocean, *Paleoceanography*, *16*, 260–267.

Minas, H. J., M. Minas, and T. T. Packard (1986), Productivity in upwelling areas deduced from hydrographic and chemical fields, *Limnol. Oceanogr.*, *31*, 1182–1206.

Mortlock, R. A., C. D. Charles, P. N. Froelich, M. A. Zibello, J. Saltsman, J. D. Hays, and L. H. Burckle (1991), Evidence for lower productivity in the Antarctic Ocean during the last glaciation, *Nature*, *351*, 220–223.

Murray, D. W. (1987), Spatial and temporal variations in sediment accumulation in the central tropical Pacific, Ph.D. thesis, 343 pp., Oregon State Univ., Corvallis.

Pedersen, T. F., B. Nielsen, and M. Pickering (1991), Timing of late quaternary productivity pulses in Panama basin an implications for atmospheric CO_2, *Paleoceanography*, *6*, 657–677.

Petit, J. R., et al. (1999), Climate and atmospheric history of the past 420,000 years from the Vostok ice core, Antarctica, *Nature*, *399*, 429–436.

Pollock, D. E. (1997), The role of diatoms, dissolved silicate and Antarctic glaciation in glacial/interglacial climate change: A hypothesis, *Global Planet. Change*, *14*, 113–125.

Ragueneau, O., et al. (2002), Direct evidence of a biologically active silicate pump: Ecological implications, *Limnol. Oceanogr.*, *47*, 1849–1854.

Shackleton, N. J. (2000), The 100,000-year ice-age cycle identified and found to lag temperature, carbon dioxide, and orbital eccentricity, *Science*, *289*, 1897–1902.

Shackleton, N. J., and N. G. Pisias (1985), Atmospheric carbon dioxide, orbital forcing, and climate, in *The Carbon Cycle and Atmospheric CO2: Natural Variations Archean to Present*, *Geophys. Monogr. Ser.*, vol. 32, edited by E. T. Sundquist and W. S. Broecker, pp. 303–317, AGU, Washington, D. C.

Sigman, D. M., and E. A. Boyle (2000), Glacial/interglacial variations in atmospheric carbon dioxide, *Nature*, *407*, 859–869.

Smetacek, V. (1985), Role of sinking in diatom life-history cycles: Ecological, evolutionary and geological significance, *Mar. Biol.*, *84*, 239–251.

Smetacek, V. (1998), Biological oceanography: Diatoms and the silicate factor, *Nature*, *391*, 224–225.

Takahashi, T., J. Goddard, S. Southerland, D. W. Chipman, and C. C. Breeze (1986), Seasonal and geographic variability of carbon dioxide sink/source in the ocean areas, *Tech. Rep. Contract MERTTA 19X.89675C*, 66 pp., Lamont-Doherty Geol. Obs., Palisades, N. Y.

Takahashi, T., R. A. Feely, R. F. Weiss, R. H. Wanninkhof, D. W. Chipman, S. C. Sutherland, and T. T. Takahashi (1997), Global air-sea flux of CO_2: An estimate based on measurements of sea-air pCO_2 difference, *Proc. Natl. Acad. Sci.*, *94*, 8292–8299.

Toggweiler, J. R., and S. Carson (1995), What are upwelling ecosystems contributing to the ocean's carbon and nutrient budgets?, in *Upwelling in the Ocean, Modern Processes And Ancient Records*, edited by C. P. Summerhayes et al., pp. 337–361, John Wiley, Hoboken, N. J.

Toggweiler, J. R., K. Dixon, and W. S. Broecker (1991), The Peru upwelling and the ventilation of the South Pacific thermocline, *J. Geophys. Res.*, *96*, 20,467–20,497.

Tréguer, P., D. M. Nelson, A. J. Van Bennekom, D. J. DeMaster, A. Leynaert, and B. Queguiner (1995), The silica balance in the world ocean: A re-estimate, *Science*, *268*, 375–379.

R. T. Barber, NSOE Marine Laboratory, Duke University, 135 Duke Marine Lab Road, Beaufort, NC 28516, USA. (rbarber@duke.edu)

F. Chai, School of Marine Science, 5471 Libby Hall, University of Maine, Orono, ME 04469-5741, USA. (fchai@maine.edu)

R. C. Dugdale and F. P. Wilkerson, Romberg Tiburon Center, San Francisco State University, 3152 Paradise Drive, Tiburon, CA 94920, USA. (rdugdale@sfsu.edu; fwilkers@sfsu.edu)

M. Lyle, Center for Geophysical Investigation of the Shallow Subsurface, Boise State University, Boise, ID 83725-1536, USA. (mlyle@boisestate.edu)

T.-H. Peng, Ocean Chemistry Division, NOAA Atlantic Oceanographic and Meteorological Laboratory, 4301 Rickenbacker Causeway, Miami, FL 33149-1026, USA. (peng@aoml.noaa.gov)